

A Search for Unbound Stellar Companions to Pulsar J1124–5916

C. S. Kochanek^{1,2}

¹ *Department of Astronomy, The Ohio State University, 140 West 18th Avenue, Columbus OH 43210*

² *Center for Cosmology and AstroParticle Physics, The Ohio State University, 191 W. Woodruff Avenue, Columbus OH 43210*

29 June 2022

ABSTRACT

We searched for and found no higher mass ($\gtrsim 3M_{\odot}$) unbound binary stellar companions to the progenitor of pulsar J1124–5916. There are lower mass candidates, but they all have high probabilities of being false positives. There are no candidates for it now being a fully unbound triple system. Even if one of the lower mass candidates is an unbound companion, it seems unlikely that it could have contributed to stripping the progenitor prior to the supernova. The stars are too low mass to be significant mass gainers, and they are too slowly moving to be the survivors of a compact, post-common envelope binary. The addition of one more system slightly improves the statistical constraints on the binary and triple status of supernova progenitors just before and after death.

Key words: stars: massive – supernovae: general – supernovae

1 INTRODUCTION

Massive stars are overwhelmingly born in binaries and higher order systems (e.g., Kobulnicky & Fryer 2007, Sana et al. 2012, Moe & Di Stefano 2017, Villaseñor et al. 2021) and this has profound effects on their evolution and ultimate fates. Predictions about their deaths in supernovae or implosion, the numbers of interacting massive compact object binaries, or gravitational wave mergers all require understanding their multiplicity and the evolution of binary systems, which can be explored in binary population synthesis models (e.g., Belczynski et al. 2002, Kalogera et al. 2007, Belczynski et al. 2008, Dominik et al. 2013, Antonini et al. 2017, Eldridge et al. 2017, Fragione & Kocsis 2019). Many of the uncertainties in these models for the fates of massive stars could be reduced given direct constraints on their multiplicity just before and after their deaths in supernovae rather than only at birth.

The multiplicity of supernovae leading to neutron stars can be well constrained using the roughly 300 Galactic supernova remnants (e.g., Green 2019) up to the limitations imposed by extinction. The original approach (van den Bergh 1980, Guseinov et al. 2005) was simply to look for O and B stars associated with supernova remnants. Surviving, bound binaries can be constrained from the optical properties of the associated compact objects (Kochanek 2018). Kochanek et al. (2019) examined 23 SNRs with known compact objects, finding three interacting binaries (the black hole Roche accretion system SS 433 (e.g., Hillwig & Gies 2008) and the wind accre-

tion systems HESS J0632+057 (Hinton et al. 2009) and 1FGL J1018.6–5856 (Corbet et al. 2011)) and no non-interacting binaries. Unbound binaries can be identified by searching for stars with proper motions that either intersect the center of the SNR or the motion of the neutron star at a reasonable look back time (Dinçel et al. 2015, Boubert et al. 2017, Fraser & Boubert 2019, Kochanek 2021, Lux et al. 2021). In particular, Kochanek (2021) surveyed 10 SNRs containing neutron stars with proper motion measurements to find only one unbound binary, the star HD 37424 in G180.0–01.7 that had been previously identified by Dinçel et al. (2015). Kochanek (2021) then combines all these available statistics to provide the first direct measurements of the binary properties of supernovae producing neutron stars: 72% are not binaries at death, 14% are bound binaries and 13% are unbound binaries after the explosion. Roughly speaking, these limits are for stars $\gtrsim 3M_{\odot}$, although individual mass limits can be significantly smaller. The statistical uncertainties are still large, but they are also only based on $\sim 10\%$ of the Galactic SNRs.

Recently, Long et al. (2022) measured a proper motion for the pulsar J1124–5916 (Hughes et al. 2001, Camilo et al. 2002) in the SNR G292.0+1.8. The separation of the pulsar from the expansion center of the SNR (Winkler et al. 2009) already implied a high velocity, and Long et al. (2022) find a velocity of 612 ± 152 km/s in the Gaia reference frame. Relative to the local standard of rest of the stars, the velocity is somewhat higher (744 km/s, see below). G292.0+1.8 is an oxygen rich SNR where the

recent X-ray abundance analysis of Bhalerao et al. (2019) suggests a progenitor mass of 13 to $30M_{\odot}$, lower than earlier estimates (Gonzalez & Safi-Harb 2003, Yang et al. 2014, Kamitsukasa et al. 2014). Temim et al. (2022) argue for an even lower progenitor mass of $12\text{--}16M_{\odot}$. The explosion has swept up a large amount of mass ($\sim 14M_{\odot}$, Chevalier 2005, Bhalerao et al. 2019) some of which lies in an “equatorial ring” (Park et al. 2007, Ghavamian, Hughes, & Williams 2005) which is interpreted as material lost by the progenitor. The lower progenitor masses combined with the large mass of circumstellar material implies that the progenitor must have been stripped by either winds or binary interactions prior to the explosion. The equatorial ring is also suggestive of the presence of a binary. Temim et al. (2022) model the SNR and are able to reproduce its properties under the assumption of a stripped progenitor exploding into a large mass of previously ejected gas.

Here we combine the Long et al. (2022) proper motion measurement with Gaia EDR3 (Gaia Collaboration et al. 2016, Gaia Collaboration et al. 2021) to search for disrupted binary or triple stellar companions to PSR J1124–5916. We summarize the data and the method developed to search for companions by Kochanek (2021) in §2. In §3 we present the results, and we discuss them in §4.

2 DATA AND METHODS

Hughes et al. (2001) identified PSR J1124–5916 as a likely pulsar in Chandra X-ray observations of the SNR G292.0+1.8. This was confirmed by Camilo et al. (2002), who found it was a 135 msec radio pulsar with a spin down age of only 2900 years. Its J2000 position is 11:24:39.0(1)–59:16:19(1) based on a Fermi LAT timing solution (Ray et al. 2011). This position is $1''.8$ from the original Chandra position. As noted earlier, Long et al. (2022) measured the proper motion of the pulsar using several epochs of Chandra observations. They report their final result as a velocity of 612 ± 152 km/s at a position angle of 126 ± 17 degrees assuming a distance of 6.2 kpc. This corresponds to a proper motion of $\mu_{\alpha} = 16.9 \pm 5.6$ mas/year and $\mu_{\delta} = -12.3 \pm 5.9$ mas/year in the Gaia reference frame.

G292.0+1.8 extends 9.6 arcmin North-South and 8.4 arcmin East-West (Park et al. 2007) so we adopt the geometric mean radius of $R_{SNR} = 4.5$ arcmin. Winkler et al. (2009) measure an expansion center of (J2000) 11:24:34.4–59:15:51 and an expansion age of 2990 ± 60 years based on the proper motions of [OIII] 5007\AA emission line filaments. The 46 arcsec offset of the pulsar from the expansion center already implied the pulsar had a high proper motion before its direct measurement.

Gaensler & Wallace (2003) estimated a minimum distance of 6.2 ± 0.9 kpc based on the observed HI absorption profile of the SNR. Goss et al. (1979) estimated a distance of 5.4 kpc based on the optical extinction of the SNR emission, and Camilo et al. (2002) estimate a distance of 5.7 kpc based on the dispersion measure and the models of Cordes & Lazio (2002). We use the distances of 5.4 kpc and 7.1 kpc to define a “pseudo-parallax” for the SNR of $\varpi = 0.16 \pm 0.02$ mas as the mean of these distances as parallaxes and their separation from the mean as the uncertainty, rounded to two digits. Goss et al. (1979) estimated that the extinction was

$E(B - V) \simeq 0.9$ mag. Gaensler & Wallace (2003) measure a hydrogen column density of $N(H) \simeq 3.3 \times 10^{21}$ cm $^{-2}$ which corresponds to $E(B - V) \simeq 0.6$ for the dust-to-gas ratio of Bohlin, Savage, & Drake (1978).

We select nearby stars from Gaia EDR3 (Gaia Collaboration et al. 2016, Gaia Collaboration et al. 2021), requiring them to have proper motions, all three Gaia magnitudes (G , B_P and R_P), $G < 19$ mag, $\varpi < 1$ mas and to lie within within 0.1° of the center of the SNR. This should include all stars more massive than approximately $2M_{\odot}$ for a distance of 6.2 kpc and $E(B - V) = 0.9$ mag. We include no restrictions on the RUWE statistic for the quality of the parallax. For the present effort we can ignore the small systematic uncertainties in the parallax zero point. We searched the Hipparcos (Perryman et al. 1997) and Bright Star (Hoffleit & Warren 1995) catalogs for any bright ($G \lesssim 3$ mag) stars that would be missing from Gaia and found none. At this point we have 3526 stars.

For extinction estimates we used the three dimensional combined19 `mw dust` models (Bovy et al. 2016), which combine the Drimmel et al. (2003), Marshall et al. (2006) and Green et al. (2019) models to provide extinction estimates for any sky position as a function of distance. We extracted the V band extinction, and use the PARSEC estimates of A_{λ}/A_V for the Gaia EDR3 bands and an $R_V = 3.1$ extinction law to convert the V band extinction to those for the G , B_P and R_P bands. At a distance of 6.2 kpc, the `mw dust` extinction estimate is $E(B - V) \simeq 0.65$ mag, and there is a rapid rise in the extinction between 3 and 5 kpc.

We used Solar metallicity PARSEC (Bressan et al. 2012, Marigo et al. 2013, Pastorelli et al. 2020) isochrones to characterize the stars. Table 1 gives rough cuts on the extinction-corrected absolute magnitude M_G as a function of color for selecting stars more massive than $3M_{\odot}$, $4M_{\odot}$ or $5M_{\odot}$. Kochanek (2021) also includes the limits for $1M_{\odot}$ and $2M_{\odot}$, but for G292.0+1.8 we are dominated by false positives even for the rarer higher mass stars. Because of the distance, most of the stars lack good parallaxes, so we use the distance corresponding to the joint parallax estimate between the star and the SNR (see below). Essentially, this will set the mass scale to the mass a star would have at the distance to the SNR.

Our approach is the same as in Kochanek (2021). We first simply identify stars whose parallaxes are consistent with the pseudo-parallax assigned to the SNR by fitting for a joint parallax and computing the χ^2_{ϖ} goodness of fit. We initially keep all stars which satisfy $\chi^2_{\varpi} < 9$. Next we identify all stars which could intersect the path of the neutron star in the time interval $-t_{max} < t_m < 0$ with a stellar velocity $v_* < v_{max}$ with $t_{max} = 10^4$ years and $v_{max} = 1000$ km/s. We allowed this very high maximum velocity because of the discussions of stripping the progenitor in a common envelope phase (e.g., Bhalerao et al. 2019, Temim et al. 2022), which can lead to a compact binary with high orbital speeds. In practice, the maximum proper motion of the $\chi^2_{\varpi} < 9$ stars is 22.8 mas/yr in the local standard of rest, or 670 km/s at 6.2 kpc. This star has a very uncertain parallax ($\varpi = 0.18 \pm 0.22$ mas) and is probably a slower moving star at a smaller distance. This step leaves 1882 stars and the N_* column of Table 2 gives the number of stars above each M_{lim} .

For these stars, we do a joint fit to the proper motions

Table 1. CMD Selection Limits

Mass	Color	Mag	Color)	Mag	Color	Mag	Color	Mag
$> 3M_{\odot}$	< 0.7	1.0	0.7-1.1	2.0	1.1-2.0	$-1 - 3(B_P - R_P - 1)$	> 2	-4
$> 4M_{\odot}$	< 0.0	0.5	0.0-1.3	-1.9	1.3-2.0	$-1 - 3(B_P - R_P - 1)$	> 2	-4
$> 5M_{\odot}$	< 0.0	-0.4	0.0-1.3	-1.9	1.3-2.0	$-1 - 3(B_P - R_P - 1)$	> 2	-4

Mag gives the upper limit on M_G for each $B_P - R_P$ color range.

Table 2. Searching For Disrupted Binaries

M_{lim} (M_{\odot})	N_*	N_{obs}	90% N_{ran}	Prob.	N_{obs}	95% N_{ran}	Prob.	N_{obs}	99% N_{ran}	Prob.
> 5	5	0	0.1	–	0	0.1	–	0	0.1	–
> 4	7	0	0.1	–	0	0.2	–	0	0.2	–
> 3	208	3	3.3	64%	5	4.8	52%	8	6.8	36%

of each star and the neutron star, introducing the “true” proper motions as variables to be fit to the observed proper motions, and penalize the separation of the star and the pulsar given the true proper motions. Thus, the fit statistic in RA for stars 1 and 2 is

$$\chi_{\alpha,12}^2 = \frac{(\mu_{\alpha,1} - \mu_{\alpha,1}^T)^2}{\sigma_{\alpha,1}^2} + \frac{(\mu_{\alpha,2} - \mu_{\alpha,2}^T)^2}{\sigma_{\alpha,2}^2} + \frac{(\Delta\alpha_{12} - t(\mu_{\alpha,1}^T - \mu_{\alpha,2}^T))^2}{\sigma_a^2} \quad (1)$$

where $\mu_{\alpha,i}$ is the measured proper motion, $\mu_{\alpha,i}^T$ is the unknown true proper motion, t is the time, and

$$\sigma_a = 10''0 \left(\frac{a_{max}}{10^4 \text{ AU}} \right) \left(\frac{\varpi}{\text{mas}} \right). \quad (2)$$

sets the scale for the maximum semi-major axis a_{max} of the binary search. Note that there is little gain from shrinking a_{max} since it is unimportant once the positional uncertainties created by the proper motions are larger than σ_a . There is also an analogous contribution $\chi_{\delta,12}^2$ for the motion in Declination and the combined statistic $\chi_{\mu}^2 = \chi_{\alpha,12}^2 + \chi_{\delta,12}^2$ can then be minimized.

We optimize χ_{μ}^2 with respect to t^{-1} . If we define $\Delta\mu_{\alpha} = \mu_{\alpha,1} - \mu_{\alpha,2}$, $\Delta\mu_{\delta} = \mu_{\delta,1} - \mu_{\delta,2}$, $\sigma_{\alpha,12}^2 = \sigma_{\alpha,1}^2 + \sigma_{\alpha,2}^2 + \sigma_a^2/t^2$ and $\sigma_{\delta,12}^2 = \sigma_{\delta,1}^2 + \sigma_{\delta,2}^2 + \sigma_a^2/t^2$ we can minimize χ_{μ}^2 analytically while holding t constant in $\sigma_{\alpha,12}$ and $\sigma_{\delta,12}$ and then iteratively update the time used in these uncertainties to deal with the intrinsic non-linearity. This then leads to a time of closest approach

$$t_m = - \frac{\Delta\alpha_{12}^2 \sigma_{\delta,12}^2 + \Delta\delta_{12}^2 \sigma_{\alpha,12}^2}{\Delta\alpha_{12} \Delta\mu_{\alpha,12} \sigma_{\delta,12}^2 + \Delta\delta_{12} \Delta\mu_{\delta,12} \sigma_{\alpha,12}^2} \quad (3)$$

with a propagation of errors uncertainty of

$$\sigma_t = t_m^2 \left(\frac{\sigma_{\alpha,12}^2 \sigma_{\delta,12}^2}{\Delta\delta_{12}^2 \sigma_{\alpha,12}^2 + \Delta\alpha_{12}^2 \sigma_{\delta,12}^2} \right)^{1/2} \quad (4)$$

and a goodness of fit of

$$\chi_{\mu}^2 = \frac{(\Delta\delta_{12} \Delta\mu_{\alpha,12} - \Delta\alpha_{12} \Delta\mu_{\delta,12})^2}{\Delta\alpha_{12}^2 \sigma_{\delta,12}^2 + \Delta\delta_{12}^2 \sigma_{\alpha,12}^2}. \quad (5)$$

The same procedure can be used to search for unbound triples and the complete expressions are given in Kochanek (2021).

It is also important to evaluate the probability of having false positives. First, we characterize the SNR by scrambling the stellar positions relative to their magnitudes, proper motions and parallaxes. The proper motion and parallax errors are largely determined by the magnitude, so these three quantities cannot be trivially scrambled. We randomly assign each star the position of a different star and count the fraction of trials which have closest approaches within 20% of the SNR radius and joint fit statistics $\chi_{\varpi}^2 + \chi_{\mu}^2$ less than several limits. This test characterizes the general false positive properties of the SNR given the available data.

Second, we evaluate the likelihood that each candidate is a false positive by taking all stars with $\chi_{\varpi}^2 < 9$ and within 1 mag of each candidate, putting them at the position of the candidate and determining the fraction of these trials which have a goodness of fit $\chi_{\varpi}^2 + \chi_{\mu}^2$ fit less than the larger of the value found for the candidate or 2.706 (90% confidence). This tests whether, for example, a candidate is simply located at a position where many randomly selected proper motions would still allow a low fit statistic. This test characterize the false positive properties of each candidate. These individual candidate probabilities can be very different than the more general false positive test above if a candidate has a very different proper motion than the typical star.

3 RESULTS

Given its space velocity and the non-mention of binarity in the pulsar timing studies, it is unlikely that the pulsar can be in a surviving binary. The optical and near-IR counterpart to the pulsar is also very faint, with combined emission from the pulsar and its wind nebula of $V = 24.3$, $R = 24.1$, $I = 23.1$, $H = 21.3$ and $K_s = 20.5$ mag (Zharikov et al. 2013). For a distance of 6.2 kpc and the `mw dust` extinction estimate of $E(B - V) = 0.65$ mag, these correspond to absolute magnitudes of $M_V = 8.3$, $M_R = 8.5$, $M_I = 7.9$, $M_H = 6.9$ and $M_{K_s} = 6.3$ mag, which limits the mass of any star associated with the pulsar to $M_* \lesssim 0.2M_{\odot}$ for a 10 million year Solar metallicity PARSEC isochrone. It would be essentially impossible to keep such a low mass star in a binary after the explosion, so it seems safe to conclude that the pulsar is no longer in a binary.

Table 3. Disrupted Binary Candidates

Gaia EDR3 ID	M_{lim} (M_{\odot})	False (%)	χ_{ϖ}^2	χ_{μ}^2	t_{min} (10^3 yr)	R/R_{SNR}	ϖ (mas)
5339171053702282112	3	98	0.591	2.083	-4.3 ± 1.0	0.27	0.153 ± 0.018
5339171019342516608	3	86	0.213	0.211	-4.5 ± 0.9	0.28	0.156 ± 0.018
5339171019342516352	3	99	3.261	0.023	-3.8 ± 0.8	0.21	0.151 ± 0.019
5339170847543846656	3	99	1.164	3.933	-3.0 ± 0.8	0.14	0.154 ± 0.019
5339170847543834240	3	100	1.058	2.133	-1.5 ± 0.3	0.02	0.156 ± 0.020
5339170847543832320	3	99	3.029	1.852	-0.9 ± 0.2	0.07	0.180 ± 0.017
5339170847543831168	3	99	0.092	0.772	-2.0 ± 0.4	0.04	0.161 ± 0.019
5339170808840074752	3	99	4.507	1.471	-1.1 ± 0.2	0.06	0.185 ± 0.016

Table 4. Properties of Candidates

Gaia EDR3 ID	χ^2/N_{dof}	$\log(T_*/K)$	$\log(L_*/L_{\odot})$	M_*/M_{\odot}	$\log t$
5339171053702282112	1.00	3.672 ± 0.020	1.512 ± 0.066	1.1-2.3	8.92-9.99
5339171019342516608	1.50	3.648 ± 0.021	1.449 ± 0.068	1.1-1.8	9.23-9.99
5339171019342516352	0.48	3.646 ± 0.024	0.938 ± 0.077	1.1-1.3	9.65-9.99
5339170847543846656	0.81	3.646 ± 0.017	0.953 ± 0.052	1.1-1.2	9.80-9.99
5339170847543834240	1.16	3.823 ± 0.019	1.305 ± 0.050	1.6-2.3	< 9.36
5339170847543832320	1.40	3.703 ± 0.027	1.640 ± 0.081	1.0-2.6	8.75-9.99
5339170847543831168	1.05	3.720 ± 0.021	0.923 ± 0.057	1.1-1.7	9.33-9.99
5339170808840074752	1.04	3.729 ± 0.032	0.949 ± 0.101	1.1-2.1	< 9.99

Fig. 1 shows the $\chi_{\varpi}^2 < 9$ stars superposed on the central region of the SNR both at their present locations and where they would have been 2000 years ago given their Gaia EDR3 proper motions. The coherent motions in the upper panel are simply due to the Galactic rotation curve and the Galactic longitude ($\ell = 292^\circ$) of the pulsar. Using the rough distances and simply assuming a flat 240 km/s rotation curve, the predicted tangential motion is roughly 170 km/s, which is 6 mas/year. The stars have mean proper motions of $(-6.4 \pm 1.9, 1.7 \pm 1.3)$ mas, where the uncertainty is the dispersion not the formal error, and the result changes little if we tighten the parallax limit. The median proper motions are $(-6.2, 1.7)$ mas/year. This mean motion of 6.6 mas/year is both parallel to the Galactic plane (see Fig. 1) and a very close match to the expectation from the simple kinematic model. There are roughly equal contributions from our motion and the local standard of rest (LSR) at the pulsar.

Fig. 1 also shows the back projection of the pulsar to 0, 1000, 2000, 3000 and 4000 years ago in the Gaia kinematic frame of reference along with the associated uncertainty given the estimated errors on the pulsar proper motions from Long et al. (2022). The errors on the pulsar proper motions completely dominate the problem: the Gaia EDR3 proper motion uncertainties are roughly 50 times smaller than those of the pulsar, and a 10^4 AU orbit only subtends only $1''.6$ at 6.2 kpc (Eqn. 2). A star in Fig. 1 would be good unbound binary candidate with an age of 2000 years if the head of its arrow lies in the corresponding pulsar error circle.

Fig. 1 also shows the motions in the local standard of rest defined by the median proper motions of the stars with $\chi_{\varpi}^2 < 9$. In this frame, the motions of the stars over 2000 years are generally negligible compared to the uncertainties in the back propagated position of the pulsar. The pulsar proper motion is now (23.1, 10.6) mas/year in-

stead of (16.9, 12.3) mas/year with the total increasing to 25.4 mas/year from 20.9 mas/year. This increases the velocity from 612 km/s to 744 km/s at a distance of 6.2 kpc. It is now quite difficult to reconcile the Winkler et al. (2009) expansion center of the SNR, the pulsar motions and an age close to 3000 years. An age of 2000 years remains acceptable.

The Gaia frame version of Fig. 1 is not fully consistent because we have presented it as if the expansion center is fixed in this frame. In reality, if the explosion is spherical and the ISM is roughly comoving with the stars, then the velocity of the expansion center is the same as the pre-SN velocity of the progenitor star. If any pre-SN orbital velocity was small, then in the Gaia frame of Fig. 1, the expansion center is moving to the South-East with roughly the median proper motions of the stars. Including this would reconcile the apparently different positions of the pulsar relative to the expansion center in the Gaia and LSR frames shown in Fig. 1.

We assume the expansion center of the SNR is at rest with respect to the LSR, and so give it the median proper motion of the stars when we compute the distance of stars from the explosion center as a function of time. While certainly wrong at some level, it is a better assumption than keeping it at rest in the Gaia frame given that there are both large differences between the Gaia frame and the LSR and that these differences have nothing to do with any physics leading to the expansion center having a motion relative to the LSR. Compared to Kochanek (2021) we also used a maximum fractional distance of the closest approach point from the expansion center of $R/R_{SNR} < 0.3$ instead of 0.2.

Table 2 provides the general false positive character of G292.0+1.8 based on randomly mixing the coordinates and proper motions. It counts the number of real and random candidates which have $R/R_{SNR} < 0.3$ at the time of

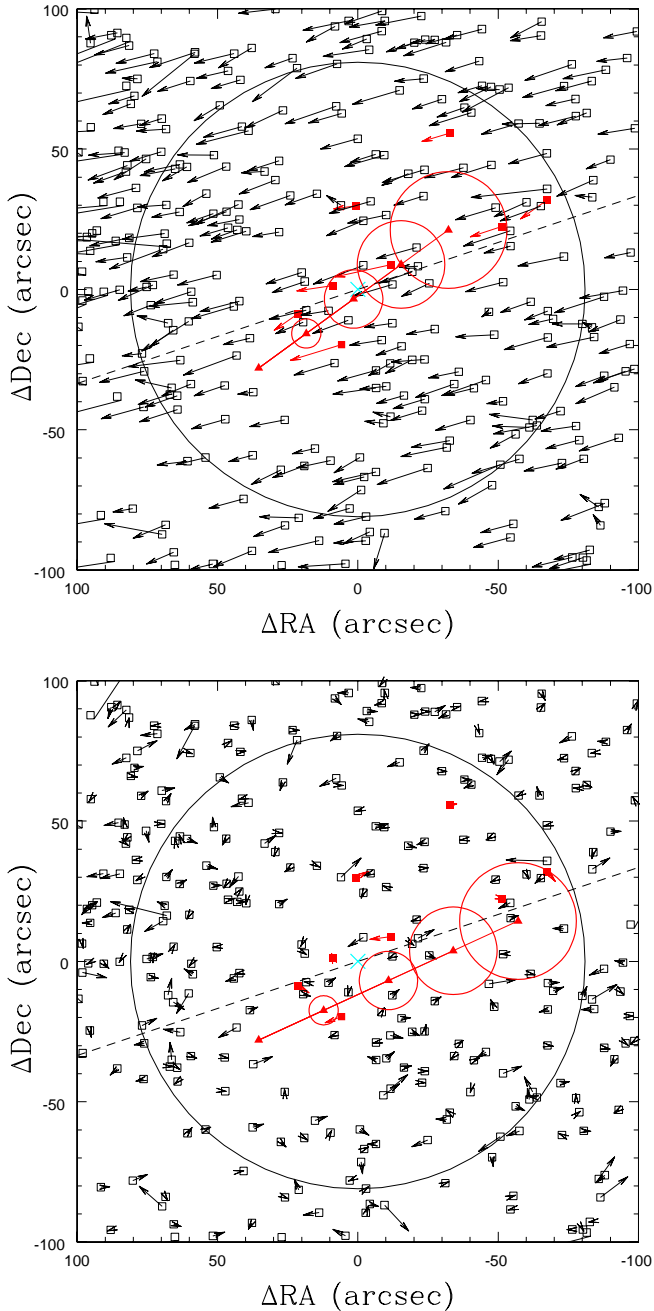


Figure 1. The motions of the pulsar and its surrounding stars in the Gaia frame (top) and the LSR (bottom) defined by the median proper motion of the stars with $\chi^2_{\text{tot}} < 9$. Squares are the current positions of the stars, and the arrows extend to their positions 2000 years ago. The eight binary candidates from Table 3 are in red. The red triangles with the growing circles show the position of the pulsar 0, 1000, 2000, 3000 and 4000 years ago with their associated (1σ) uncertainties shown by the red circles. Positions are relative to the Winkler et al. (2009) expansion center, which is marked by the cyan cross. The large black circle corresponds to 30% of the mean radius of the SNR around the expansion center. We only include stars presently in the region or there 2000 years ago. The dashed line is parallel to the Galactic plane, and we see that the Gaia frame proper motions are roughly parallel to the plane because they are dominated by the effects of the Galactic rotation curve.

closest approach and $\chi^2_{\text{tot}} + \chi^2_{\mu} < 2.71$, 3.84, or 6.64, corresponding to probabilities that 90%, 95% and 99% of systems should have smaller fit statistics. Clearly, the probability of candidates being false positives is high given the proper motion statistics and their uncertainties. In essence, the proper motions of the stars are all pretty similar, particularly compared to the uncertainties in the pulsar proper motions. So using the proper motions of a randomly selected star has very little effect on whether a given stellar coordinate will produce a good candidate. Visually, if a star in Fig. 1 can lie inside the pulsar error circle at some time, it is highly likely to do so no matter which arrow is assigned to it.

All the individual candidates with $M_{\text{lim}} > 3M_{\odot}$, $\chi^2_{\text{tot}} + \chi^2_{\mu} < 6.64$ and $R/R_{\text{SNR}} < 0.3$ are listed in Table 3, along with their individual false positive rate estimates, the times of closest approach, the distances from the expansion center R/R_{SNR} at that time and the joint parallaxes of the star and the SNR. These eight candidates are marked in Fig. 1. As discussed in §2, the individual false positive rate is the probability that the star would still be a candidate if we give it the proper motion of a randomly selected star within 1 mag of its observed magnitude. These are all essentially 100%, which is again a manifestation of the similarity of the stellar proper motions relative to the uncertainties in the pulsar proper motion. There are increasing numbers of candidates for larger ages because the area of the pulsar error circle grows quadratically with time (Fig. 1), limited only by when significant fractions of the error circle begin to be too far from the expansion center ($R/R_{\text{SNR}} > 0.3$) at the time of closest approach. If we keep the expansion center position fixed in the Gaia frame, the number of candidates increases significantly because it takes longer for the pulsar to approach the $R/R_{\text{SNR}} < 0.3$ limit. We used fairly generous age, goodness of fit and R/R_{SNR} limits for Table 3, and we could reasonably prune the list by tightening the limits. However, even the remaining candidates would still be ambiguous because of the high false positive probabilities.

We can conclude, however, that any former stellar companion cannot have been a massive star. To better quantify this than the crude M_{lim} values, we made spectral energy distribution (SED) models using Castelli & Kurucz (2003) stellar atmospheres for the eight stars in Table 3 using AllWISE W_1/W_2 (Cutri et al. 2021), 2MASS JHK_s (Skrutskie et al. 2006), and ATLAS Refcat griz (Tonry et al. 2018) photometry. We use either the reported photometric error or a minimum error of 0.1 mag to account for systematic uncertainties (e.g., metallicity etc.). We fixed the distance to 6.2 kpc and used an extinction prior of $E(B - V) = 0.65 \pm 0.10$ based on the *mwdust* extinction estimate for that distance.

Table 4 gives the results. They are all relatively cool stars (4700 K to 6400 K) with luminosities of $10L_{\odot}$ to $62L_{\odot}$. The fitted extinctions are broadly consistent with the prior, although most stars want modestly lower extinctions. Forcing the extinction to be $E(B - V) = 0.65$ mag does not significantly alter the results. We matched the luminosities and temperatures to Solar metallicity PARSEC isochrones using minimum luminosity and temperature uncertainties of 0.1 and 0.05 dex, respectively, finding the mass and age ranges consistent ($\chi^2 < 4$) with the luminosity and temperature estimates. The stars appear to be moderately evolved 1.0 to $2.6M_{\odot}$ stars, although we suspect that they are mostly

lower luminosity main sequence stars with overestimated luminosities from placing them at 6.2 kpc. That the masses are lower than the $M_{lim} > 3M_{\odot}$ limit is not an issue – these limits are designed to be very conservative.

4 DISCUSSION

The current proper motion uncertainties for the pulsar prevent us from providing an unambiguous answer for the pre-supernova binary status of PSR J1124–5916. There are 8 candidate stars with various levels of plausibility, all of which have very high false positive properties. We suspect, but cannot prove, that they are all false positives. The Long et al. (2022) proper motions measurements used Chandra data spanning 2006 to 2016, so it is already feasible to reduce the proper motion uncertainties by 50%, which would significantly reduce the false positive problem. There are no candidates for a fully disrupted triple system.

All eight of the stars are relatively low mass, $< 3M_{\odot}$, so none could be a significant (relative to the initial mass of a neutron star progenitor) mass gainer. They also all have relatively low proper motions (see Fig. 1), so none are candidates for a disrupted, short period post-common envelope binary. If the progenitor of PSR J1124–5916 was a highly stripped star, as argued by Bhalariao et al. (2019) and Temim et al. (2022), it seems unlikely that it was stripped by binary interactions.

We can also update the binary status probabilities of neutron star producing SN from Kochanek (2021). With the addition of this system, we have 10 systems which were not binaries with $M \gtrsim 3M_{\odot}$ companions at death, 1 unbound binary, 2 interacting binaries (this assume SS 433 is a black hole system), and 11 which are not bound binaries but could be unbound binaries. If $f_n = 1 - f_u - f_b$ is the fraction that are not binaries at the time of the SN, f_u is the fraction producing unbound binaries, fraction $f_b = f_i + f_p$ are bound binaries after the SN with f_i interacting and f_p non-interacting (passive), then the joint multinomial probability is

$$f_n^{10} (1 - f_b)^{11} f_u f_i^2$$

from which we can compute the median and 90% confidence limits on the terms given in Table 5. There is an ambiguity from Kochanek et al. (2019) about whether interacting binaries are so easy to detect that the two in the sample were all the interacting binaries in the parent sample of 49 SNRs they considered. If this is true, then the joint multinomial probability should be

$$f_n^{10} (1 - f_b)^{11} (1 - f_i)^{20} f_u f_i^2.$$

This case is given in the “non-interacting complete” columns. Adding a single system does not change the the from Kochanek (2021) results significantly, but it shows that steady progress can be made in observationally determining all of these parameters. Adding this system, there are 11 systems which are not fully unbound triples, so of systems not leaving a bound binary, $< 17.5\%$ can be fully unbound triples at 90% confidence.

As noted earlier, there are roughly 300 known Galactic SNRs, and this statistical analysis makes use of only $\sim 10\%$ of them. If the statistics used in Eqn. 4 could simply be

doubled, the constraints on binary properties improve dramatically. For example, if we literally simply double each exponent in Eqn. 4, the uncertainty in the fraction of systems which are binaries at death drops from 55%-87% (Table 5) to 65%-88%. and the error on the fraction in bound binaries drops from 5%-26% to 5%-19%. Much of this can be done with added studies like Long et al. (2022) to measure the proper motions of known compact objects. Proper motions can also help to identify the compact objects in SNRs where there are multiple X-ray sources since active galactic nuclei, the primary contaminant, have no proper motions. It is, however, necessary to obtain such observations with Chandra because of its superior angular resolution to other existing and planned X-ray missions. As we have already noted in Kochanek (2021) and Kochanek (2022) combining Gaia stellar distances with searches for high velocity stellar absorption features from the SNR, as done by Cha et al. (1999) for the Vela remnant, should provide a means of obtaining more accurate distances to SNRs. Poor SNR distances are one of the main contributors to false positives.

ACKNOWLEDGMENTS

CSK is supported by NSF grants AST-1814440 and AST-1907570. This work has made use of data from the European Space Agency (ESA) mission *Gaia* (<https://www.cosmos.esa.int/gaia>), processed by the *Gaia* Data Processing and Analysis Consortium (DPAC, <https://www.cosmos.esa.int/web/gaia/dpac/consortium>). Funding for the DPAC has been provided by national institutions, in particular the institutions participating in the *Gaia* Multilateral Agreement. This research has made use of the SIMBAD database, operated at CDS, Strasbourg, France

DATA AVAILABILITY STATEMENT

All data used in this paper are publicly available.

REFERENCES

- Antonini, F., Toonen, S., & Hamers, A. S. 2017, ApJ, 841, 77.
- Belczynski, K., Kalogera, V., & Bulik, T. 2002, ApJ, 572, 407.
- Belczynski, K., Kalogera, V., Rasio, F. A., et al. 2008, ApJS, 174, 223
- Bhalariao J., Park S., Schenck A., Post S., Hughes J. P., 2019, ApJ, 872, 31
- Bohlin R. C., Savage B. D., Drake J. F., 1978, ApJ, 224, 132
- Boubert, D., Fraser, M., Evans, N. W., Green, D. A., & Izzard, R. G. 2017, AAP, 606, A14
- Bovy, J., Rix, H.-W., Green, G. M., et al. 2016, ApJ, 818, 130
- Bressan, A., Marigo, P., Girardi, L., et al. 2012, MNRAS, 427, 127
- Camilo F., Manchester R. N., Gaensler B. M., Lorimer D. R., Sarkissian J., 2002, ApJL, 567, L71

Table 5. Constraints on Binaries

Case	Non-Interacting Incomplete		Non-Interacting Complete	
	Median	90% Confidence	Median	90% Confidence
Not Binary at Death	73.5%	54.6%-87.2%	77.4%	58.4%-89.7%
Bound Binary	13.4%	5.2%-26.3%	9.2%	3.5%-19.2%
Interacting Binary	9.8%	3.1%-21.5%	5.6%	1.8%-12.8%
Non-Interacting Binary		<8.2%		<8.6%
Unbound Binary	11.6%	2.6%-29.2%	12.2%	2.7%-30.6%

- Castelli, F., & Kurucz, R. L. 2003, *Modelling of Stellar Atmospheres*, 210, 20P
- Cha, A. N., Sembach, K. R., & Danks, A. C. 1999, *ApJL*, 515, L25.
- Chevalier R. A., 2005, *ApJ*, 619, 839.
- Corbet, R. H. D., Cheung, C. C., Kerr, M., et al. 2011, *The Astronomer’s Telegram*, 3221,
- Cordes J. M., Lazio T. J. W., 2002, *arXiv*, astro-ph/0207156
- Cutri R. M., Wright E. L., Conrow T., Fowler J. W., Eisenhardt P. R. M., Grillmair C., Kirkpatrick J. D., et al., 2021, *yCat*, II/328
- Dinçel, B., Neuhäuser, R., Yerli, S. K., et al. 2015, *MNRAS*, 448, 3196
- Dominik, M., Belczynski, K., Fryer, C., et al. 2013, *ApJ*, 779, 72.
- Drimmel, R., Cabrera-Lavers, A., & López-Corredoira, M. 2003, *AAP*, 409, 205
- Eldridge, J. J., Stanway, E. R., Xiao, L., et al. 2017, *PASA*, Fragione, G. & Kocsis, B. 2019, *MNRAS*, 486, 4781.
- Fraser, M., & Boubert, D. 2019, *ApJ*, 871, 92
- Gaensler B. M., Wallace B. J., 2003, *ApJ*, 594, 326
- Gaia Collaboration, Prusti, T., de Bruijne, J. H. J., et al. 2016, *AAP*, 595, A1
- Gaia Collaboration, Brown, A. G. A., Vallenari, A., et al. 2021, *AAP*, 649, A1
- Ghavamian P., Hughes J. P., Williams T. B., 2005, *ApJ*, 635, 365.
- Gonzalez M., Safi-Harb S., 2003, *ApJL*, 583, L91
- Goss W. M., Shaver P. A., Zealey W. J., Murdin P., Clark D. H., 1979, *MNRAS*, 188, 357
- Green, G. M., Schlafly, E., Zucker, C., et al. 2019, *ApJ*, 887, 93
- Green, D. A. 2019, *Journal of Astrophysics and Astronomy*, 40, 36.
- Guseinov, O. H., Ankay, A., & Tagieva, S. O. 2005, *Astrophysics*, 48, 330
- Hillwig, T. C., & Gies, D. R. 2008, *ApJL*, 676, L37
- Hinton, J. A., Skilton, J. L., Funk, S., et al. 2009, *ApJL*, 690, L101
- Hoffleit, D. & Warren, W. H. 1995, *VizieR Online Data Catalog*, V/50x
- Hughes J. P., Slane P. O., Burrows D. N., Garmire G., Nousek J. A., Olbert C. M., Keohane J. W., 2001, *ApJL*, 559, L153
- Kalogera, V., Belczynski, K., Kim, C., et al. 2007, *Physics Reports*, 442, 75.
- Kamitsukasa F., Koyama K., Tsunemi H., Hayashida K., Nakajima H., Takahashi H., Ueda S., et al., 2014, *PASJ*, 66, 64
- Kobulnicky, H. A., & Fryer, C. L. 2007, *ApJ*, 670, 747
- Kochanek, C. S. 2018, *MNRAS*, 473, 1633
- Kochanek, C. S., Auchettl, K., & Belczynski, K. 2019, *MNRAS*, 485, 5394
- Kochanek C. S., 2021, *MNRAS*, 507, 5832
- Kochanek C. S., 2022, *MNRAS*, 511, 3428.
- Long X., Patnaude D. J., Plucinsky P. P., Gaetz T. J., 2022, *arXiv*, arXiv:2205.07951
- Lux, O., Neuhäuser, R., Mugrauer, M., et al. 2021, *Astronomische Nachrichten*, 342, 553.
- Marigo, P., Bressan, A., Nanni, A., et al. 2013, *MNRAS*, 434, 488
- Marshall, D. J., Robin, A. C., Reylé, C., et al. 2006, *AAP*, 453, 635
- Marshall, H. L., Canizares, C. R., Hillwig, T., et al. 2013, *ApJ*, 775, 75
- Moe, M., & Di Stefano, R. 2017, *ApJS*, 230, 15
- Park S., Hughes J. P., Slane P. O., Burrows D. N., Gaensler B. M., Ghavamian P., 2007, *ApJL*, 670, L121
- Pastorelli, G., Marigo, P., Girardi, L., et al. 2020, *MNRAS*, 498, 3283
- Perryman, M. A. C., Lindegren, L., Kovalevsky, J., et al. 1997, *AAP*, 500, 501
- Ray P. S., Kerr M., Parent D., Abdo A. A., Guillemot L., Ransom S. M., Rea N., et al., 2011, *ApJS*, 194, 17
- Sana, H., de Mink, S. E., de Koter, A., et al. 2012, *Science*, 337, 444
- Skrutskie, M. F., Cutri, R. M., Stiening, R., et al. 2006, *AJ*, 131, 1163
- Temim T., Slane P., Raymond J. C., Patnaude D., Murray E., Ghavamian P., Renzo M., et al., 2022, *ApJ*, 932, 26
- Tonry J. L., Denneau L., Flewelling H., Heinze A. N., Onken C. A., Smartt S. J., Stalder B., et al., 2018, *ApJ*, 867, 105
- van den Bergh, S. 1980, *Journal of Astrophysics and Astronomy*, 1, 67
- Villaseñor, J. I., Taylor, W. D., Evans, C. J., et al. 2021, *arXiv*:2107.10170
- Winkler P. F., Twelker K., Reith C. N., Long K. S., 2009, *ApJ*, 692, 1489
- Yang X.-J., Liu X.-Q., Li S.-Y., Lu F.-J., 2014, *RAA*, 14, 1279-1288.
- Zharikov S. V., Zyuzin D. A., Shibanov Y. A., Mennickent R. E., 2013, *A&A*, 554, A120